

# Strong Coupling of Multimolecular Species to Soft Microcavities

Adarsh B. Vasista\* and William L. Barnes\*



Cite This: *J. Phys. Chem. Lett.* 2022, 13, 1019–1024



Read Online

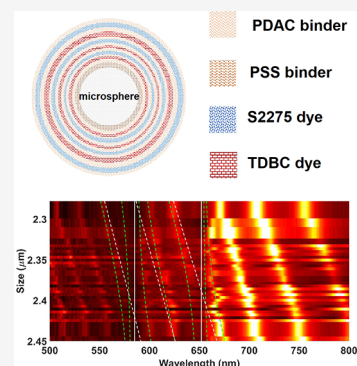
ACCESS |

Metrics & More

Article Recommendations

Supporting Information

**ABSTRACT:** Can we couple multiple molecular species to soft cavities? The answer to this question has relevance in designing open cavities for polaritonic chemistry applications. Because of the differences in adhesiveness, it is difficult to couple multiple molecular species to open cavities in a controlled and precise manner. In this Letter, we discuss the procedure to coat multiple dyes, TDBC and S2275, onto a dielectric microsphere using a layer-by-layer deposition technique so as to facilitate the multimolecule coupling. We observed the formation of a middle polariton branch due to the intermolecular mixing facilitated by the whispering gallery modes. The coupling strength,  $2g$ , of the TDBC molecules was found to be 98 meV, while that of the S2275 molecules was 78 meV. The coupling strength was found to be greater than the cavity line width and the molecular absorption line width, showing that the system is in the strong coupling regime.



Coupling molecules to cavities has wide implications in controlling molecular properties.<sup>1,2</sup> If the molecule–cavity coupling strength is greater than the losses in the system, then the system is said to be in the strong coupling regime, where new energy eigenstates are created.<sup>3</sup> These new states derive their properties from both the cavity and the molecule, thus acting as a platform to engineer optical,<sup>4,5</sup> electronic,<sup>6</sup> and chemical properties<sup>7</sup> of the hybrid system. Various cavity architectures have been studied in the context of strong coupling, such as Fabry–Perot cavities,<sup>8</sup> gap plasmon cavities,<sup>9</sup> and single nanostructures.<sup>10</sup> A recent development in the field of molecular strong coupling is the use of dielectric cavities in place of metallic ones.<sup>11–13</sup> Dielectric cavities provide sharper cavity resonances and do not suffer from Joule heating losses. Among the different classes of dielectric cavities, microspheres—also called *soft cavities*—have gained prominence recently.<sup>14</sup>

Soft cavities belong to the class of open cavities, and they can be easily fabricated and functionalized, are biocompatible, and can be used in microfluidic environments. They support spectrally sharp resonances called whispering gallery modes (WGMs). Dielectric soft cavities have been shown to influence molecular emission by changing the polarization and the direction of the emission.<sup>15</sup> They have also been used to detect single molecules,<sup>16</sup> and to strongly couple a molecular monolayer.<sup>14</sup>

In the past, Fabry–Perot cavities<sup>8</sup> and nanoparticles<sup>17</sup> have been utilized to couple multiple molecular species, thereby facilitating intermolecular coupling. Such intermolecular coupling is important in harnessing the potential of strong coupling, particularly in areas such as long-range energy transfer<sup>18</sup> and polariton lasing.<sup>19</sup> To be able to couple multiple molecular species, coupling must take place over an extended spectral range, which can be achieved in two ways. First, a wide spectral

range can be achieved if the optical mode employed is also broad, as is the case for example with (nondispersive) particle plasmon resonances. However, the wider line width of these particle modes poses significant limitations on the coupling strength. Second, relatively sharp optical modes can be used provided they span a wide range as a result of their dispersion, as is the case for the modes of a Fabry–Perot cavity. However, such modes are “closed” and do not provide dynamic access to the molecular medium. In this context, soft cavities have an advantage because they are open cavities and support multiple spectrally sharp resonances.

With this in mind, we studied strong coupling of layers of two dye molecules, J-aggregated 5,5,6,6-tetrachloro-1,1-diethyl-3,3-bis(4-sulfobutyl)benzimidazolocarboyanine (TDBC) and 5-chloro-2-[3-[5-chloro-3-(4-sulfobutyl)-3H-benzothiazol-2-ylidene]propenyl]-3-(4-sulfobutyl)benzothiazol-3-ium hydroxide, inner salt, triethylammonium salt (S2275), to individual microspheres with a size of  $\sim 2 \mu\text{m}$ .

A schematic of the system under study is shown in Figure 1. We consider individual polystyrene microspheres with a size of  $\sim 2 \mu\text{m}$  coated with a mixture of S2275 and TDBC dye molecules. The microsphere was placed on a glass doveprism and excited using wideband illumination through the substrate. The evanescent-based illumination excites WGMs inside the microsphere. The scattered light from the sphere in the air

**Received:** November 9, 2021

**Accepted:** December 20, 2021

**Published:** January 21, 2022



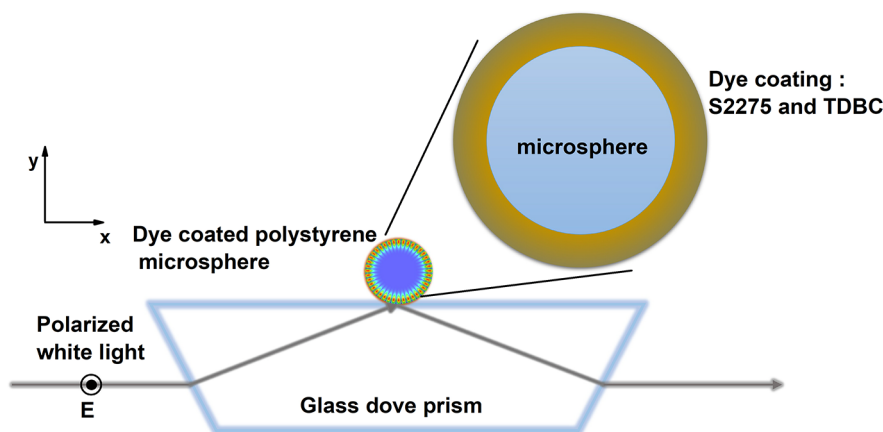


**Figure 1.** Schematic of the experiment. Individual microspheres were coated with two dye molecules, S2275 and TDBC, consecutively using a layer-by-layer approach. The molecule-coated microspheres were then probed optically using evanescent excitation and dark-field microscopy.

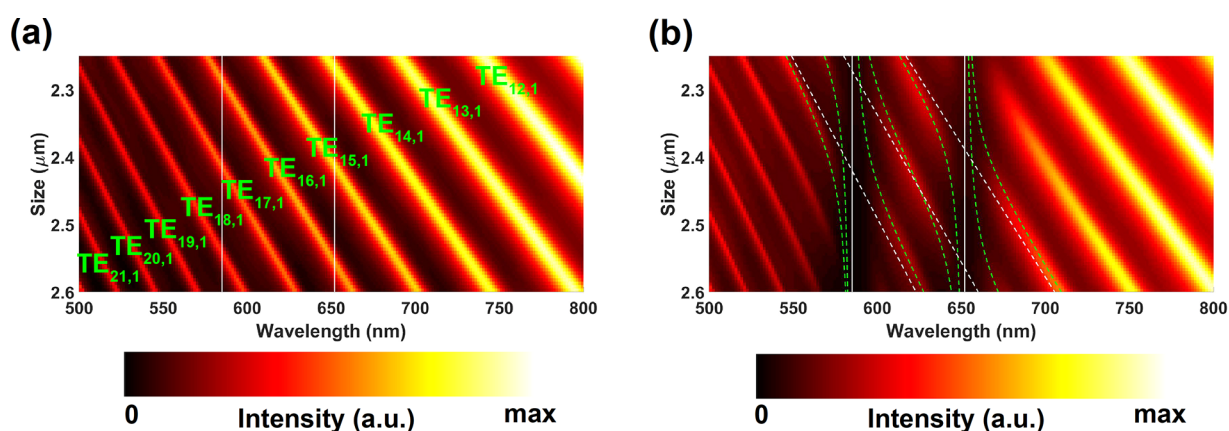


**Figure 2.** (a) Numerically calculated dispersion of WGMs of bare  $\sim 2 \mu\text{m}$  microspheres placed on a glass substrate. (b) Numerically calculated dispersion of WGMs of  $\sim 2 \mu\text{m}$  microspheres coated with three layers of S2275 and TDBC molecules. The superimposed dashed green lines represent the eigenvalues of the Hamiltonian calculated to fit the experimental and numerical data. The dashed white lines represent the uncoupled WGM, and the solid white lines represent molecular resonances.

medium was captured and analyzed, and the results are discussed below. We first performed finite-element method (FEM)-based numerical simulations to understand the molecule–WGM coupling using COMSOL Multiphysics. The wavelength-dependent refractive index of the polystyrene microsphere was taken from the literature.<sup>20</sup> The dye coating was modeled as a set of Lorentzian oscillators with permittivity  $\epsilon_{\text{dye}}$  given by

$$\epsilon_{\text{dye}}(E) = \epsilon_{\text{inf}} + \sum_{j=\text{TDBC}, \text{S2275}} \frac{f_j E_j^2}{E_j^2 - E^2 - iE\gamma_j} \quad (1)$$

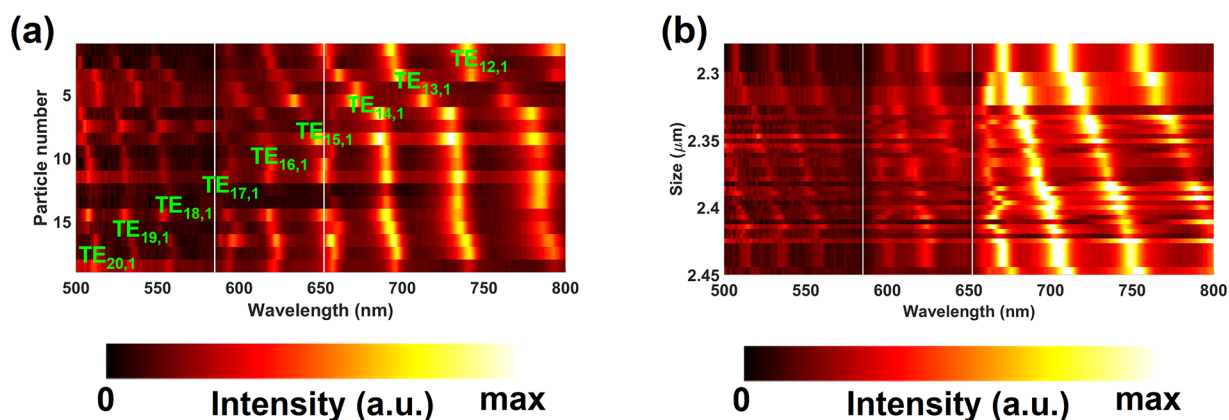
where  $\epsilon_{\text{inf}}$  is the background permittivity (set to 1.9),  $E_j$  is the resonance energy of the dye ( $E_{\text{TDBC}} = 2.1139 \text{ eV}$  and  $E_{\text{S2275}} = 1.90160 \text{ eV}$ ),  $f_j$  is the reduced oscillator strength ( $f_{\text{TDBC}} = 0.3$  and  $f_{\text{S2275}} = 0.15$ ), and  $\gamma_j$  is the resonance line width of the dye ( $\gamma_{\text{TDBC}} = 53 \text{ meV}$  and  $\gamma_{\text{S2275}} = 67 \text{ meV}$ ). The value of  $f$  was adjusted to match the experimental data. The molecular coating was considered to be homogeneous and 12 nm thick (each layer of the dye was taken to be 2 nm thick).<sup>14,21</sup>

Figure 2a shows the numerically calculated dispersion of the scattering spectra of uncoated individual microspheres. The spectrally sharp WGMs of the microsphere are clearly evident. Each WGM is characterized by two mode numbers ( $m, n$ ). The azimuthal mode number  $m$  is half the number of electric field

maxima along the periphery of the sphere, while the radial mode number  $n$  is the total number of electric field maxima along the radius of the sphere (see ref 14 for more details on assigning the mode numbers.) The polarization of light was kept as transverse electric (TE). Figure 2b shows the dispersion of individual microspheres coupled to three layers of poly-(diallyldimethylammonium chloride) (PDAC)/TDBC and S2275 dye. We can clearly see that the modes  $\text{TE}_{17,1}$ ,  $\text{TE}_{16,1}$ , and  $\text{TE}_{15,1}$  were affected by the presence of the molecular absorption. New energy eigenstates called polaritons were formed by mixing multiple WGMs and molecular resonances through the molecule–WGM coupling.

The Hamiltonian of the total system can be written as<sup>22</sup>

$$\mathcal{H} = \bigoplus_{j=1}^3 \begin{pmatrix} E_{\text{PDAC/TDBC}} & 0 & -g_{j,\text{TDBC}} \\ -i\frac{\gamma_{\text{PDAC/TDBC}}}{2} & & \\ 0 & E_{\text{S2275}} - i\frac{\gamma_{\text{S2275}}}{2} & -g_{j,\text{S2275}} \\ -g_{j,\text{TDBC}} & -g_{j,\text{S2275}} & E_j - i\frac{\gamma_j}{2} \end{pmatrix} \quad (2)$$



**Figure 3.** (a) Experimentally measured dispersion of the microspheres coated with the mixture of S2275 and TDBC dye molecules. The size of the microspheres was  $\sim 2 \mu\text{m}$ . (b) Experimentally measured dispersion of the microspheres coated with alternating layers of S2275 and TDBC molecules. The solid white lines represent the positions of molecular resonances.

where  $E_j$  represents the energy of the  $j$ th WGM of the resonator and  $\gamma_j$  represents its line width. The eigenvalues of eq 2 give us the polariton energies, while the eigenvectors provide an estimate of the mixing fractions (Hopfield coefficients). We fit the numerical simulation data with the eigenvalues from eq 2, and the results are superimposed on Figure 2b. The values of the coupling strengths were found to be  $g_{\text{TE}_{17,1}, \text{PDAC/TDBC}} = 46 \text{ meV}$ ,

$g_{\text{TE}_{17,1}, \text{S2275}} = 0 \text{ meV}$ ,  $g_{\text{TE}_{16,1}, \text{PDAC/TDBC}} = 49 \text{ meV}$ ,  $g_{\text{TE}_{16,1}, \text{S2275}} = 39 \text{ meV}$ ,  $g_{\text{TE}_{15,1}, \text{PDAC/TDBC}} = 0 \text{ meV}$ , and  $g_{\text{TE}_{15,1}, \text{S2275}} = 39 \text{ meV}$ . In the

cases where WGMs interact with the molecular resonance ( $\text{TE}_{17,1}$  with PDAC/TDBC,  $\text{TE}_{15,1}$  with S2275, and  $\text{TE}_{16,1}$  with PDAC/TDBC and S2275), the coupling strength,  $2g$ , was found to be greater than the mean of the coupling molecular resonance line width ( $\gamma_{\text{TDBC}} = 53 \text{ meV}$ ,  $\gamma_{\text{S2275}} = 67 \text{ meV}$ ) and the WGM line width ( $\gamma_{\text{TE}_{17,1}} = 13 \text{ meV}$ ,  $\gamma_{\text{TE}_{16,1}} = 15 \text{ meV}$ ,  $\gamma_{\text{TE}_{15,1}} = 21 \text{ meV}$ ), indicating that the strong coupling regime has been reached.<sup>23</sup>

This shows that soft cavities support spectrally sharp resonances that can be utilized to strongly couple multiple molecular species.

Having established strong coupling of multimolecular species to soft cavities numerically, we now focus on the experimental implementation using a layer-by-layer deposition (LBL) method. In a typical deposition step, we mixed  $20 \mu\text{L}$  of anionic polystyrenesulfonate (PSS) solution (20% by weight in water, diluted 1:1000) with 1 mL of polystyrene microsphere colloidal solution (15% by weight in water, diluted 1:50), and the resulting solution was allowed to settle for 20 min. The solution was then washed three times in water to remove excess polyelectrolyte solution. This step was followed by mixing with the cationic polyelectrolyte PDAC (20% by weight in water, diluted 1:1000), and the resulting solution was also allowed to settle for 20 min. The solution was washed three times in water to remove excess polyelectrolyte. The dye mixture was prepared by mixing 0.5 mL of 0.01 M TDBC solution and 0.5 mL of 0.01 M S2275 solution. Then  $40 \mu\text{L}$  of this dye mixture was mixed with the solution of polyelectrolyte-coated microspheres, and the resulting mixture was allowed to settle for 20 min. The solution was washed with water three times to remove excess dye solution. This step was repeated with PDAC as a binder layer a further five times.

The individual dye-coated microspheres were then probed using evanescent excitation in a dark-field configuration. White

light was used to excite WGMs of the microsphere, and the scattered light was then collected using a 0.8 NA, 100 $\times$  objective lens. To obtain a dispersion plot, we collected spectral signatures from multiple microspheres, each with a slightly different size, and then ordered the spectra in ascending order of the size of the microspheres (see section S1 in the Supporting Information for details of the experimental setup). We excited the spheres with TE-polarized light, as the deposited molecular layers show zero radial dipole moment and hence the transverse-magnetic-polarized scattering shows no signs of molecule–cavity coupling.<sup>14</sup>

Figure 3a shows the experimentally measured dispersion of the microspheres after they were coated with the mixture of dyes. The dispersion plot was created by arranging individual dark-field scattering spectra from 20 microspheres in ascending order. We can see that the WGM in resonance with TDBC absorption ( $\text{TE}_{17,1}$ ) was perturbed by TDBC–cavity coupling. However, the mode resonant with S2275 absorption ( $\text{TE}_{15,1}$ ) shows almost no change. This clearly shows that mixing two dyes to form a solution and then coating the mixture on a microsphere does not yield multimolecule–cavity coupling. We suggest that this happens because of the different polarities of the dyes. LBL is a charge-based deposition technique in which the anionic dye layer is deposited as a result of the electrostatic attraction between the polyelectrolyte binder and the dye. The total charge carried by TDBC dominates the dye mixture, and hence, TDBC is selectively adsorbed on the microsphere. Thus, we see a molecule–cavity coupling signature only from TDBC and not from S2275. It should be noted that it is difficult to calculate the exact size of the microspheres, in this case, by fitting the measured spectra because of the unknown percentages of S2275 and TDBC molecules adsorbed on the microspheres; that is why the dispersion is shown as a function of particle number. However, the overall message of molecule–cavity coupling can be conveyed effectively using particle number rather than size.

To solve the problem of adhesiveness, we modified the deposition procedure by alternately depositing TDBC and S2275 molecules on the microsphere. The polyelectrolyte-deposited microsphere solution was mixed with  $20 \mu\text{L}$  of 0.01 M TDBC dye solution and allowed to settle for 20 min. The solution was then washed in water three times to remove excess TDBC molecules. Next, a layer of PDAC as a binding layer was deposited using the procedure described earlier. Then we mixed  $20 \mu\text{L}$  of 0.01 M S2275 dye solution and allowed it to settle for

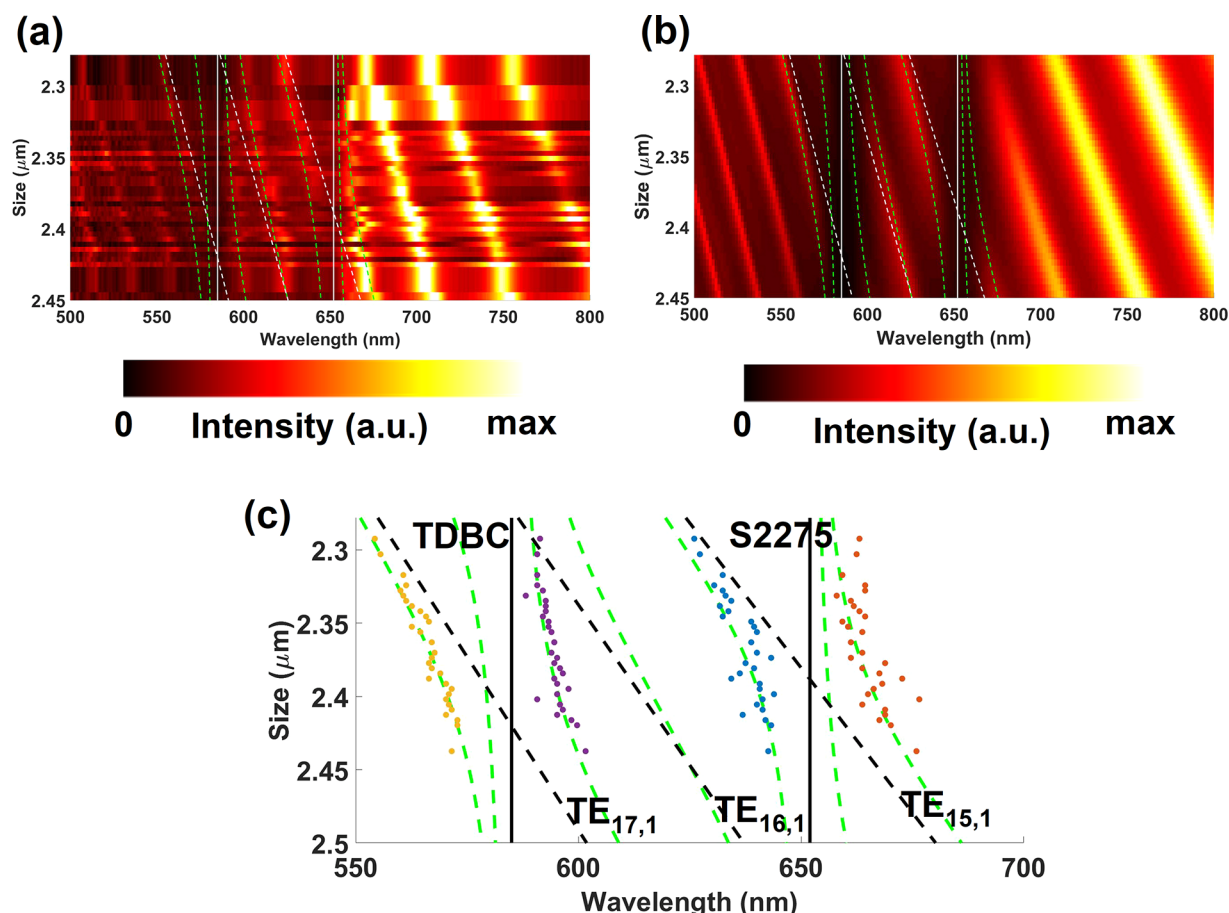


**Figure 4.** (a) Experimentally measured dispersion of WGMs of  $\sim 2 \mu\text{m}$  microspheres coated with three layers of S2275 and TDBC molecules. (b) Numerically calculated dispersion of WGMs of  $\sim 2 \mu\text{m}$  microspheres coated with three layers of S2275 and TDBC molecules. The superimposed dashed green lines represent the eigenvalues of the Hamiltonian calculated to fit the experimental and numerical data. The dashed white lines represent the uncoupled WGM, and the solid white lines represent molecular resonances. (c) Calculated dispersion plot of the modes  $\text{TE}_{15,1}$ ,  $\text{TE}_{16,1}$ , and  $\text{TE}_{17,1}$  using a coupled oscillator model to fit to the experimental data. The experimental values of the spectral positions of the lower and upper polaritons were extracted from (a) and are represented as dots. The dashed green lines are the fits using a coupled oscillator model.

20 min. The solution was then washed in water three times to remove excess dye molecules. This procedure was repeated to deposit three layers of TDBC and S2275 each. Dye-coated microspheres were then drop-cast on a glass substrate and probed with evanescent excitation dark-field spectroscopy.

Figure 3b shows the experimentally measured dispersion of the WGMs of microspheres after they were coated with alternating layers of dye molecules. Now, in contrast to Figure 3a, we can see splitting and anticrossing of modes  $\text{TE}_{15,1}$  and  $\text{TE}_{17,1}$ , which are resonant with S2275 and TDBC absorption, respectively. The sizes of the microspheres in this case were calculated by fitting the measured scattering spectra with the numerically calculated spectra. To further analyze the coupling of the two types of dye molecules to an individual microsphere, we fit the experimental data with a simple coupled oscillator model, given by eq 2, as shown in Figure 4a.

The size range of the available microspheres was restricted (see Figures 2 and 4) because of manufacturing limitations. Nonetheless, we can see clear splitting and anticrossing of the modes  $\text{TE}_{17,1}$  and  $\text{TE}_{15,1}$  that are spectrally resonant with the molecular absorptions of the PDAC/TDBC and S2275 dye molecules, respectively. Figure 4b shows the nice match between the numerically calculated dispersion for the size range of 2.25–2.45  $\mu\text{m}$  and the experimental data. We have superimposed the calculated eigenvalues of the Hamiltonian on the experimental

data in Figure 4a. We used the same parameters for the Hamiltonian to fit the experimental and the numerical data. A discussion of the mixing fractions, also called Hopfield coefficients, is given in section S2 in the Supporting Information. The widths of the lower polariton branch (LPB) and the upper polariton branch (UPB) created as a result of the strong coupling of TDBC molecules to  $\text{TE}_{17,1}$  were found to be  $23 \pm 1$  and  $34 \pm 1$  meV, respectively. In the case of polaritons formed as a result of strong coupling of  $\text{TE}_{15,1}$  to S2275, the width of the LPB was found to be  $30 \pm 1$  meV, and that of UPB was found to be  $35 \pm 1$  meV. We calculated the widths of the polariton branches by fitting the scattering spectra of the microsphere with a size of 2.34  $\mu\text{m}$ . To make the strong coupling of multimolecular species to WGMs clearer, we extracted the spectral positions of the LPB and the UPB from Figure 4a and plotted them as functions of the size of the microspheres in Figure 4c. We also fit the experimental data using the coupled oscillator Hamiltonian defined in eq 2. Figure 4c clearly shows the splitting and anticrossing between the polariton branches.

Similar results have been obtained with the Fabry–Perot resonators<sup>8</sup> and with nanoparticles.<sup>17</sup> An important difference between Fabry–Perot resonators and soft cavities is that the former show well-defined angular dispersion of the modes while the latter have no angular dispersion. In the case of soft cavities, the dispersion of the modes is a *collective* effect defined by the

size variation of the resonator (as the spectral positions of the WGMs are size-dependent). Since we chose to work with a single microsphere, in any given implementation we probed only a limited part of the total range of mixing fractions, unlike the case for the Fabry–Perot resonator. This indicates that the equivalence of size in the case of soft cavities with the angle of incidence in the Fabry–Perot resonators is not a complete equivalence.

To summarize, we have numerically and experimentally demonstrated strong coupling of multiple molecular species with dielectric soft cavities through dark-field scattering signatures. We used the layer-by-layer deposition method to accurately control the molecular deposition on the microspheres. We also discussed the procedure to deposit multiple dyes onto the microspheres to facilitate multimolecule strong coupling. We anticipate that these results will find relevance in the design of open cavities for polariton-mediated multimolecular interactions such as energy transfer, lasing, etc. As the microspheres can be trapped and moved in a microfluidic environment, the results discussed here can be extrapolated to achieve multimolecule strong coupling in a dynamic microfluidic environment.

## ■ ASSOCIATED CONTENT

### SI Supporting Information

The Supporting Information is available free of charge at <https://pubs.acs.org/doi/10.1021/acs.jpcllett.1c03678>.

Additional experimental details, including a schematic of the setup and a discussion of the Hopfield coefficients (PDF)

Transparent Peer Review report available (PDF)

## ■ AUTHOR INFORMATION

### Corresponding Authors

**Adarsh B. Vasista** – Department of Physics and Astronomy, University of Exeter, Exeter EX4 4QL, United Kingdom; Nanophotonic Systems Laboratory, ETH Zurich, 8092 Zurich, Switzerland; [orcid.org/0000-0001-7641-8647](https://orcid.org/0000-0001-7641-8647); Email: [avasista@ethz.ch](mailto:avasista@ethz.ch)

**William L. Barnes** – Department of Physics and Astronomy, University of Exeter, Exeter EX4 4QL, United Kingdom; [orcid.org/0000-0002-9474-5534](https://orcid.org/0000-0002-9474-5534); Email: [w.l.barnes@exeter.ac.uk](mailto:w.l.barnes@exeter.ac.uk)

Complete contact information is available at: <https://pubs.acs.org/doi/10.1021/acs.jpcllett.1c03678>

### Notes

The authors declare no competing financial interest. Research data are available from the University of Exeter repository (<https://doi.org/10.24378/exe.3763>).

## ■ ACKNOWLEDGMENTS

The authors acknowledge the support from the European Research Council through the Photmat Project (ERC-2016-AdG-742 222; <http://www.photmat.eu>). A.B.V. thanks Wai Jue Tan and Kishan Menghrajani for their help in the preparation of the samples.

## ■ REFERENCES

(1) Pelton, M. Modified Spontaneous Emission in Nanophotonic Structures. *Nat. Photonics* **2015**, *9*, 427–435.

(2) Ebbesen, T. W. Hybrid Light–Matter States in a Molecular and Material Science Perspective. *Acc. Chem. Res.* **2016**, *49*, 2403–2412.

(3) Törmä, P.; Barnes, W. L. Strong Coupling Between Surface Plasmon Polaritons and Emitters: A Review. *Rep. Prog. Phys.* **2015**, *78*, 013901.

(4) Wersäll, M.; Cuadra, J.; Antosiewicz, T. J.; Balci, S.; Shegai, T. Observation of Mode Splitting in Photoluminescence of Individual Plasmonic Nanoparticles Strongly Coupled to Molecular Excitons. *Nano Lett.* **2017**, *17*, 551–558.

(5) Ramezani, M.; Halpin, A.; Fernández-Domínguez, A. I.; Feist, J.; Rodríguez, S. R.-K.; García-Vidal, F. J.; Gómez Rivas, J. Plasmon-Exciton-Polariton Lasing. *Optica* **2017**, *4*, 31–37.

(6) Orgiu, E.; George, J.; Hutchison, J. A.; Devaux, E.; Dayen, J. F.; Doudin, B.; Stellacci, F.; Genet, C.; Schachenmayer, J.; Genes, C.; et al. Conductivity in Organic Semiconductors Hybridized with the Vacuum Field. *Nat. Mater.* **2015**, *14*, 1123–1129.

(7) Thomas, A.; Lethuillier-Karl, L.; Nagarajan, K.; Vergauwe, R. M. A.; George, J.; Chervy, T.; Shalabney, A.; Devaux, E.; Genet, C.; Moran, J.; et al. Tilting a Ground-state Reactivity Landscape by Vibrational Strong Coupling. *Science* **2019**, *363*, 615–619.

(8) Coles, D. M.; Somaschi, N.; Michetti, P.; Clark, C.; Lagoudakis, P. G.; Savvidis, P. G.; Lidzey, D. G. Polariton-mediated Energy Transfer Between Organic Dyes in a Strongly Coupled Optical Microcavity. *Nat. Mater.* **2014**, *13*, 712–719.

(9) Chikkaraddy, R.; de Nijs, B.; Benz, F.; Barrow, S. J.; Scherman, O. A.; Rosta, E.; Demetriadou, A.; Fox, P.; Hess, O.; Baumberg, J. J. Single-molecule Strong Coupling at Room Temperature in Plasmonic Nanocavities. *Nature* **2016**, *535*, 127–130.

(10) Zengin, G.; Wersäll, M.; Nilsson, S.; Antosiewicz, T. J.; Käll, M.; Shegai, T. Realizing Strong Light–Matter Interactions between Single-Nanoparticle Plasmons and Molecular Excitons at Ambient Conditions. *Phys. Rev. Lett.* **2015**, *114*, 157401.

(11) Wang, S.; Raziman, T. V.; Murai, S.; Castellanos, G. W.; Bai, P.; Berghuis, A. M.; Godiksen, R. H.; Curto, A. G.; Gómez Rivas, J. Collective Mie Exciton-Polaritons in an Atomically Thin Semiconductor. *J. Phys. Chem. C* **2020**, *124*, 19196–19203.

(12) Heilmann, R.; Väkeväinen, A. I.; Martikainen, J.-P.; Törmä, P. Strong Coupling between Organic Dye Molecules and Lattice Modes of a Dielectric Nanoparticle Array. *Nanophotonics* **2020**, *9*, 267–276.

(13) Tserkezis, C.; Gonçalves, P. A. D.; Wolff, C.; Todisco, F.; Busch, K.; Mortensen, N. A. Mie Excitons: Understanding Strong Coupling in Dielectric Nanoparticles. *Phys. Rev. B* **2018**, *98*, 155439.

(14) Vasista, A. B.; Barnes, W. L. Molecular Monolayer Strong Coupling in Dielectric Soft Microcavities. *Nano Lett.* **2020**, *20*, 1766–1773.

(15) Vasista, A. B.; Tiwari, S.; Sharma, D. K.; Chaubey, S. K.; Kumar, G. V. P. Vectorial Fluorescence Emission from Microsphere Coupled to Gold Mirror. *Adv. Opt. Mater.* **2018**, *6*, 1801025.

(16) Vollmer, F.; Arnold, S. Whispering-gallery-mode Biosensing: Label-free Detection Down to Single molecules. *Nat. Methods* **2008**, *5*, 591–596.

(17) Melnikau, D.; Govyadinov, A. A.; Sánchez-Iglesias, A.; Grzelczak, M.; Nabiev, I. R.; Liz-Marzán, L. M.; Rakovich, Y. P. Double Rabi Splitting in a Strongly Coupled System of Core–Shell Au@Ag Nanorods and J-Aggregates of Multiple Fluorophores. *J. Phys. Chem. Lett.* **2019**, *10*, 6137–6143.

(18) Georgiou, K.; Jayaprakash, R.; Othonos, A.; Lidzey, D. G. Ultralong-Range Polariton-Assisted Energy Transfer in Organic Microcavities. *Angew. Chem., Int. Ed.* **2021**, *60*, 16661–16667.

(19) Akselrod, G. M.; Young, E. R.; Bradley, M. S.; Bulović, V. Lasing through a Strongly-coupled Mode by Intra-cavity Pumping. *Opt. Express* **2013**, *21*, 12122–12128.

(20) Sultanova, N.; Kasarova, S.; Nikolov, I. Dispersion Properties of Optical Polymers. *Acta Phys. Polym., A* **2009**, *116*, 585–587.

(21) Bradley, M. S.; Tischler, J. R.; Bulović, V. Layer-by-Layer J-Aggregate Thin Films with a Peak Absorption Constant of 106 cm<sup>−1</sup>. *Adv. Mater.* **2005**, *17*, 1881–1886.

(22) Richter, S.; Michalsky, T.; Fricke, L.; Sturm, C.; Franke, H.; Grundmann, M.; Schmidt-Grund, R. Maxwell Consideration of

Polaritonic Quasi-particle Hamiltonians in Multi-level Systems. *Appl. Phys. Lett.* **2015**, *107*, 231104.

(23) Khitrova, G.; Gibbs, H. M.; Kira, M.; Koch, S. W.; Scherer, A.

Vacuum Rabi Splitting in Semiconductors. *Nat. Phys.* **2006**, *2*, 81–90.